

Article

Wheel-Based MDM-PON System Incorporating OCDMA for Secure Network Resiliency

Meet Kumari ¹, Vivek Arya ^{2,*} and Hamza Mohammed Ridha Al-Khafaji ^{3,*}

¹ Department of Electronics and Communication Engineering, Chandigarh University, Mohali 140413, Punjab, India; meet.e8072@cumail.in

² Department of Electronics and Communication Engineering, FET, Gurukula Kangri (Deemed to Be University), Haridwar 249404, Uttarakhand, India

³ Biomedical Engineering Department, Al-Mustaqbal University College, Hillah 51001, Babil, Iraq

* Correspondence: vivek.arya@gkv.ac.in (V.A.); hamza.alkhafaji@uomus.edu.iq (H.M.R.A.-K.)

Abstract: Wheel-based network resilience passive optical network (PON) based on mode division multiplexing (MDM) can be integrated with optical code division multiple access (OCDMA) schemes efficiently for the fixed and backhaul traffic under normal and break/failure fiber operating conditions. In this work, a bidirectional 10/2.5 Gbit/s hybrid MDM-OCDMA-PON system using multi-weight zero cross-correlation (MWZCC) code is proposed. Donut modes 0 and 1 are incorporated by the MDM technique in the proposed system. The benefit of this work is to offer an inexpensive, high-bandwidth and advanced long-haul network with satisfactory resource utilization ability for fiber links with protection against faults and to improve the reliability along with survivability of the network. The simulation results show the successful realization of the multimode fiber (MMF) link at 1.6 km in the uplink and 1.2 km in the downlink directions under an acceptable bit error rate (BER). The minimum accepted received power of -31 dBm in uplink and -27 dBm in downlink over 1 km link at 10/2.5 Gbit/s rate is obtained. Moreover, the minimum received power of -20 dBm in uplink and -30 dBm downlink is achieved by using MWZCC code compared to other codes handling 58 simultaneous end users. Further, the influence of fiber impairments and connected devices on the proposed approach is numerically evaluated. Moreover, it is shown that the wheel based proposed approach performs well than other topologies for the bidirectional network resilience transmission.

Keywords: mode division multiplexing (MDM); donut modes; optical code division multiple access (OCDMA); multimode fiber (MMF)



Citation: Kumari, M.; Arya, V.; Al-Khafaji, H.M.R. Wheel-Based MDM-PON System Incorporating OCDMA for Secure Network Resiliency. *Photonics* **2023**, *10*, 329. <https://doi.org/10.3390/photonics10030329>

Received: 15 February 2023

Revised: 7 March 2023

Accepted: 17 March 2023

Published: 19 March 2023



Copyright: © 2023 by the authors. Licensee MDPI, Basel, Switzerland. This article is an open access article distributed under the terms and conditions of the Creative Commons Attribution (CC BY) license (<https://creativecommons.org/licenses/by/4.0/>).

1. Introduction

The fortified multimedia applications, in addition to wider bandwidth appeal and real-time service, request immense rise in the intercommunication area. This incites service suppliers to find a highly effective method to meet the access arena requirements, which eradicates network failure and distance. Previous research has been interested in the passive optical network (PON) to address the “last mile” obstruction matter in the future generation of fiber access networks. PON does not incorporate active components with the signal pathway and is designed for point-to-multipoint. PON supplies the privilege, comprising coverage to long-reach transmission, wider bandwidth and reduced fiber deployment within the loop and local exchange. Moreover, PON network incorporation permits several splitting points that offer various customers access to the flexible topology. The hybrid topology is based on wavelength division multiplexing (WDM), time division multiplexing (TDM), optical code division multiple access (OCDMA) and orthogonal frequency division multiplexing (OFDM) [1,2].

Recently, TDM-based PON standards, such as gigabit ethernet PON (GE-PON) and gigabit PON (G-PON), are major in distinct countries. However, due to the whole bandwidth

range being shared among different customers in the system, every customer receives access to a restricted transmission rate, frequently condensed to Mbit/s. Presently, the request for large bandwidth is growing quickly because of the advent of modern multimedia apps such as video-on-demand services with online gaming. Thus, upgrading and developing the latest technologies is essential to adapt to the latest applications. Amongst the several PON technologies, time and wavelength division multiplexing PON (TWDM-PON) has been chosen as the preferred topology for next-generation PON (NG-PON) as it sustains backward compatibility, static sharing and flexibility. Additional advantages consist of a high transmission rate, stability, protocol transparency, cost-effectiveness and dedicated connectivity [3,4].

Though, multipoint transmission is handled by some addressing prime factors such as network resilience and failure management. Several approaches were presented for TWDM-PON to form possible communication, such as tree, bus, ring and wheel-based structures. Conventionally, the TWDM-PON is utilized in a tree or bus fashion. However, a link break or failure can interrupt the whole network by deactivating the optical line terminal (OLT) from optical network units (ONUs). The majority of limitations emerge from the topology of the network and be unsuccessful to employ the possible network resources effectively from mildly loaded, idle channels or customers to the highly loaded channels in the PON network. Additionally, the growing demands for huge bandwidth to handle upcoming heavy data traffic of the network access domain cannot be obtained along with the incorporation of conventional tree-based TWDM-PON. Furthermore, mapping a multi-star architecture in TWDM-PON is accessible by implanting a sequence of power splitters. The primary disadvantage of utilizing single star-based TWDM-PON is high preliminary installation expenditure because of the integration of multiplexer (MUX) and de-multiplexer (DEMUX) for each star. Moreover, ring topology was presented to reduce the cost of settling superfluous paths in conventional PONs. However, ring-based TWDM-PON generates needed reliability at average costs, and the inclusion of passive optical couplers between OLT and various ONU units raises critical power problems which inhibit the network capacity. Additionally, the hybrid topologies, i.e., the mixture of tree-star, tree-ring, ring-star or star-tree-ring, improvised TWDM-PON network capacity, redundancy and credibility while strengthening the network complexity. The recent work focuses on investigating and profiting from reliable topologies, especially for TWDM-PON, to build reliability in fast access networks. In wheel-based TWDM-PON architecture, an OLT is located in the fiber ring center linked with an ' n ' number of ONUs to generate a closed-loop access ring structure. In contrast to ring topology, OLT directly links the entire connected remote nodes (RNs) or ONUs by assigning two directed optical fiber links. This topology is employed to manage the optical and wireless resources with separate integration of each bandwidth allocation in PON [1].

1.1. Related Work

Recently, several researchers presented their proposed systems and experimental/simulation results on PON employing different topologies. Gong, Y. et al. demonstrated a WDM-PON using ring topology to analyze the system reliability and network scalability. It was found that a maximum of eight remote nodes can be connected with a receiver sensitivity of -26 dBm [5]. Yeh, C.H. et al. investigated a tree-based PON employing self-restorable apparatus against the optical fiber cable. It was found that restoration time and protection of the PON can be obtained within 7 ms [6]. Bulu, I. and Caglayan, H. presented an experimental demonstration of ring-based PON utilizing asymmetric passive splitters. It was reported that the designed network could offer full restoration of the traffic if one OLT failed in real applications [7]. Singh, S. and Singh, S. proposed a hybrid ring-tree topology in a WDM system with polarization shift keying/non-return to zero (NRZ) at 60 Gbit/s data rate for 64 consumers. The results depict that the performance of the system is affected by input signal power, channel spacing and data rate. Moreover, the orthogonal modulation format enhances the system performance in terms of high bandwidth for future

access networks [8]. Bala, A. and Dewra, S. investigated the performance of a hybrid ring-star-based dense wavelength division multiplexing (DWDM) system utilizing add/drop multiplexers. The results show that the suggested system runs a high transmission range of 150 km at a 15 Gbit/s data rate for 128 end users [9]. Rani, A. and Dewra, S. investigated the semiconductor optical amplifier (SOA) 400 mA biased current-based performance of ring and bus topologies supporting 100 nodes at 10 Gbit/s [10]. Additionally, in [11], a dual ring-based WDM system employing hybrid fiber/free space optics (FSO) link over 5 km transmission distance at 20 Gbit/s data rate was proposed. Moreover, a ring-based integrated WDM-TDM PON over 20 km single mode fiber (SMF) at 10 Gbit/s was reported [12]. In another work, a self-protected integrated FSO-fiber link-based WDM-PON system over 25 km SMF and 2 m FSO range at 24.3 Gbit/s transmission rate was successfully presented [13]. Furthermore, due to the faster development over the last few years, the SMF-based transmission system has progressively arrived at its Shannon capacity limit [14–16]. To further enhance the system capacity by keeping less extensive inline devices such as optical amplifiers, etc., for minimal cost and energy consumption/bit, mode division multiplexing (MDM) technique employing multimode fiber (MMF) or few-mode fiber (FMF) has recently been demonstrated and comprehensively reported [17]. In the MDM technique, a single fiber is utilized for transmitting distinct optical spatial modes via the single core fiber. It can also encourage the transmission abilities of fiber by ‘*n*’ times. The TWDM-PON employing MDM can be further engaged to widen the network capacity for a definite set of channels to implement the high-speed PONs [18]. Chen, Y. et al. suggested a four channels MDM-PON system employing self-homodyne detection. The results show that the suggested system delivers a high transmission rate of 160 Gbit/s over 55 km FMF successfully [19]. Moreover, Chen, Y. et al. presented a bidirectional MDM-TDM PON using a reflective semiconductor optical amplifier (RSOA) over 10 km FMF and 20 km SMF at 10 Gbit/s transmission rate [20]. Additionally, Sharma, A. et al. proposed a four-channel WDM-MDM PON using two linearly polarized (LP) modes over 10 km MMF at a 25 Gbit/s data rate [18]. Hu, T. et al. experimentally demonstrated a full-duplex PON-MDM transmission system using two LP modes over 10 km two-mode fiber at 10 Gbit/s data rate [21]. In [22], they also proposed an MDM-GPON incorporating 10 km wavelength insensitive weakly coupled FMF and 10 km SMF at a 2.5 Gbit/s transmission rate. Ren, F. et al. experimentally demonstrated an MDM-TDM-PON system using two LP modes over 10 km SMF and 10 km FMF at 10 Gbit/s data rate [23]. Wan, Y. et al. reported a chaotic power division multiplexing-based MDM-PON system over 5 km FMF at a 30 Gbit/s transmission rate [24]. Chaudhary, S. et al. presented a radio over free space optics (RoFSO) employing an MDM-WDM system over 80 km FSO at 120 Gbit/s transmission rate [25].

Furthermore, spectral amplitude coding (SAC) based OCDMA operates at bit rate instead of chip rate and balanced detection scheme to reduce the multiple access interference (MAI). SAC-OCDMA also offers a large code set at a lower cost as compared to the OCDMA scheme, which is appropriate for PON applications, where the number of users and cost are important. Moreover, it is known that by incorporating balanced detection techniques and spectral encoding in MDM-PON systems, MAI can be fully restrained. Lately, researchers have introduced various SAC-based OCDMA codes such as random diagonal (RD) [26], modified double weight (MDW) [27], optical orthogonal [28], modified frequency hopping (MFH) [29], multi diagonal (MD) [30], zero cross correlation (ZCC), etc. A Hermite–Gaussian (HG) modes OCDMA-MDM system using RD code over 11 km MMF at 100 Gbit/s transmission rate was successfully introduced in [31]. Moreover, an integrated MDM-OCDM system incorporating LP modes over 2 km two-mode fiber (TMF) at 80 Gbit/s data rate was demonstrated [32]. In another work, LP modes incorporated MDM-based OCDMA-PON system at 2 km and 40 km TMF and single mode fiber, respectively, at 80 Gbit/s transmission rate, was demonstrated [33].

1.2. Motivation and Contributions

Considering the large investments needed for MDM-PON transmission systems, using a defined topology would be of foremost significance. Moreover, except for the quality of service, complexity, power management, cost of bandwidth, defect detection, and management are challenging and critical for various service suppliers. A consumer at each receiver end in the network expects to acquire the highest bandwidth at an acceptable cost, but the conventional PON-MDM network topologies offer confined protection. The condition causes serious information loss because of failure in optical fiber medium or optical components. So, a required topology design that solves network resilience is crucial while keeping a uniform traffic transmission at a preferable and economic capacity. In one of the recent works in reference [34], ring-based PON and FSO using single weight ZCC code over 10 km fiber and 40 km FSO range at 1 Tbit/s bit rate has been suggested. Work in this reference offers high security, high data rate and long distance but lacks system scalability and supports less number of end users/nodes. Moreover, it poses high transmission losses due to the presence of unguided FSO links, such as weather and turbulence effects. Thus, there is a need for an adequate topology to overcome all these problems. Although the current developments in TWDM-PON defined the significance of ring, bus, tree, star and wheel-based topologies, no work investigated their credibility toward fault detection or failure management. Furthermore, an OCDMA is one of the promising candidates for NG-PONs. Thus, a study regarding the high-speed and secure wheel-based MDM-PON incorporating OCDMA technique for network resiliency in next future networks is needed.

In this work, an MDM-based TWDM-PON system employing the SAC-OCDMA code is demonstrated. Donut modes 0 and 1 are utilized in the proposed system to transmit 10/2.5 Gbit/s bit rate per channel over bidirectional MMFs in wheel topology. Multi-weight zero cross-correlation (MWZCC) code is utilized to minimize the MAI effect and improve network security with ' n ' input channels. Additionally, the system performance has been evaluated in terms of received optical power and bit error rate (BER). The presence of fiber impairments and the presence of noise due to various active or passive devices cause degradation in system performance. Therefore, in addition to the design and simulation analysis, the impacts of four-wave mixing (FWM), fiber interference and dispersion, power dissipation due to power splitters/combiners, and mode selectors on the proposed scheme are discussed.

This proposed work in the paper is organized as follows: Section 2 depicts the proposed design of wheel-based MDM-PON using MWZCC code. Section 3 describes the results and discussion. Section 4 concludes the work and its pros/cons and emphasizes future directions.

2. Proposed Design

Figure 1 illustrates the conceptual diagram of wheel-based architecture, first proposed by Zentani, A. in [1], which incorporates MDM-based TWDM-PON. OLT in the design is positioned in the mid of the fiber ring linked by the ' n ' number of RNs, which are further connected to the ' $2n$ ' number of connected ONUs to build a close-loop across the optical ring with end nodes.

Here, the defined wavelengths λ_n are assigned for downlink and uplink transmission to each RN with donut modes 0 and 1. OLT helps to identify, control and communicate inter RNs. Each RN is further connected to two ONUs through a fiber link, each at a single wavelength but with two different donut modes. At each RN in wheel topology, the broadcasting, completion, regeneration and rebroadcasting of wavelength for the OLT path is performed clockwise via a unidirectional ring. Moreover, in the wheel-PON architecture, the OLT is fixed with an n -secure number of transmitters (Tx) and receivers (Rx) employing an OCDMA code. Each RN is connected with a pair of ONUs working on distinct modes at each Tx/Rx as well as the same defined wavelength is used to handle the downlink and uplink traffic through two fixed fiber links. Additionally, switches are positioned with OLT to transfer the data to the respective queue, as decided by a scheduler for distinct data

conditions. In this architecture, the fiber capacity is utilized under the link failure scenario. The wheel topology directs the data from the failed/break path onto the alternative linked path that mainly encloses the OLT channel or nearby RN or ONU to reduce the failure consequences [1,35,36].

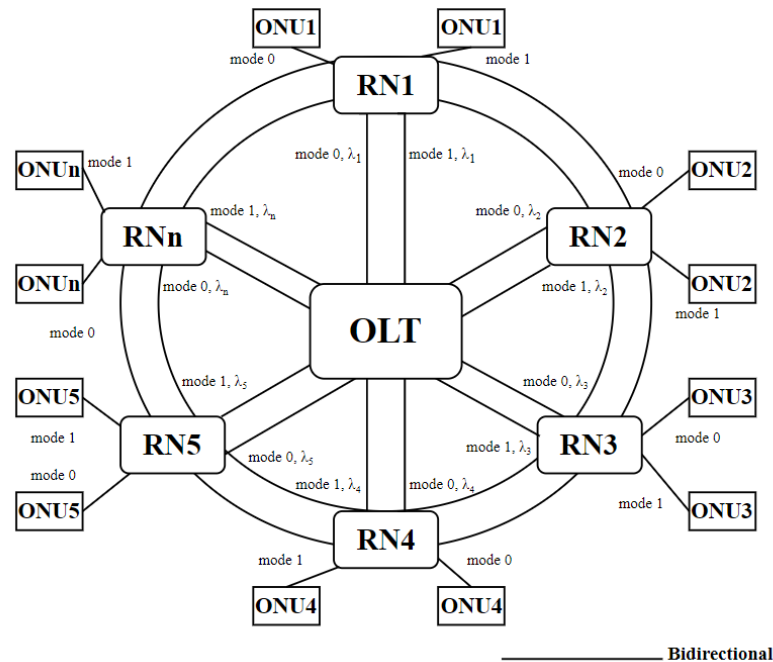


Figure 1. Conceptual diagram of network resilience wheel-based hybrid MDM-OCDMA-PON using modes 0 and 1.

Figures 2–5 illustrate the block diagram of the proposed bidirectional MDM-PON system by incorporating MWZCC OCDMA code with generated modes. In the proposed system, there are ‘*n*’ numbers of channels with a group of eighteen channels working at two MWZCC code patterns for two users. For the downlink, at the transmitter side, a continuous wave (CW) laser array operating at 10 dBm input power was utilized. Here, a single CW laser array generates eighteen wavelengths of 1596–1602.8 nm with 0.4 nm channel spacing, as depicted in Figure 2. An ideal 18:1 WDM MUX multiplexes all incoming input signals and transfers to the 1:18 WDM DEMUX in each downstream transmitter (Tx dn1). Each encoder incorporates a 4:1 WDM MUX to multiplex distinct input wavelengths according to MWZCC code sequence, pseudo-random bit sequence generator (PRBS) at 10 Gbit/s to induce a random bit sequence, a pulse generator non-return to zero and Mach Zehnder modulator (MZM) for modulating the MWZCC coded signal. The output of MZM is transferred to the mode generator that yields the donut mode 0. Likewise, in another encoder, the next coded modulated signals are transmitted to the donut mode generator that yields the donut mode 1. Afterward, a 2:1 power combiner was incorporated to join the incoming different modes signals. An *n*:1 power combiner was then used to transmit the ‘*n*’ number of transmitters (Tx dn_1 to Tx dn_n) followed by a 3-port optical circulator to direct the different incoming modes downstream signals for propagation via bidirectional MMF using two ports. The third port of the circulator was used for upstream transmission at OLT. The generated modes 0 and 1 are presented in Figures 3 and 4, respectively. Two separate MMFs are used for uplink and downlink transmission simultaneously, as depicted in Figure 5.

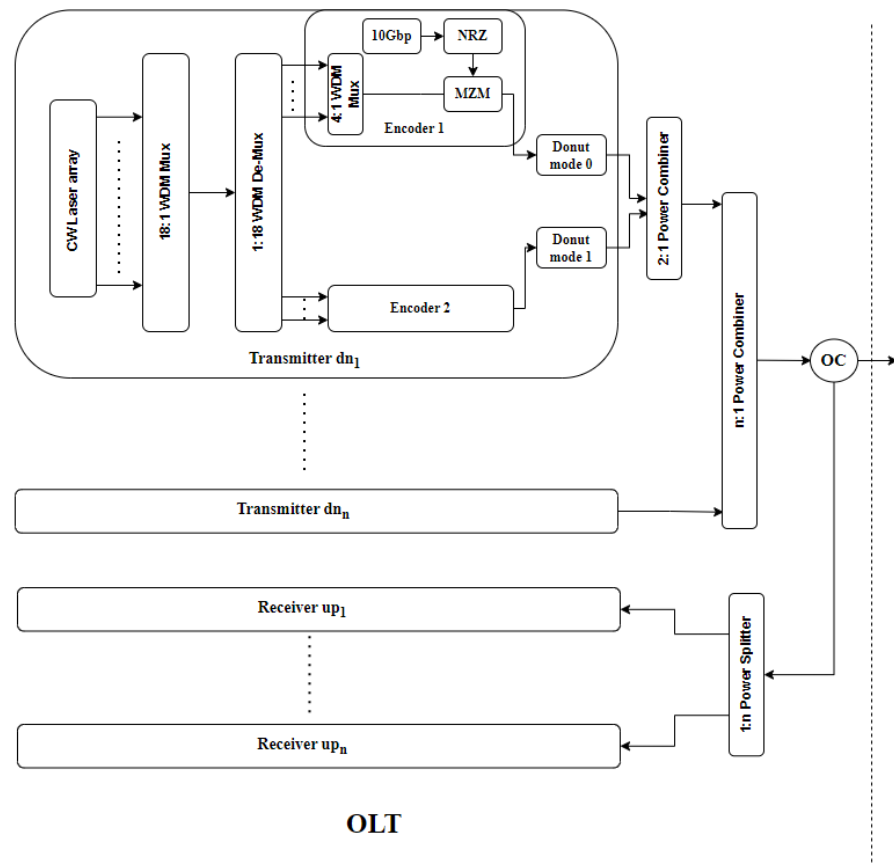


Figure 2. Proposed design of bidirectional MDM-PON system incorporating MWZCC OCDMA code of transmitter section.

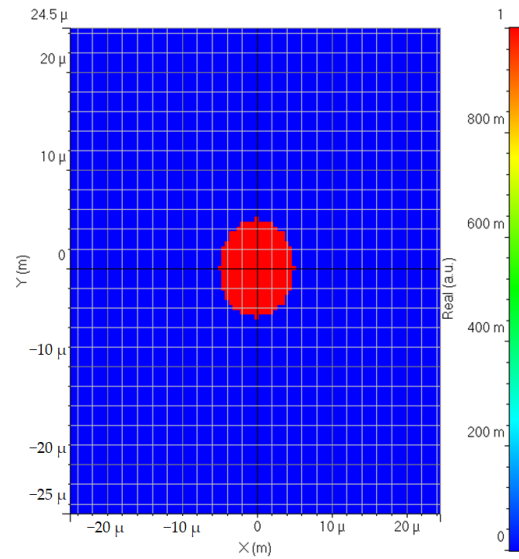


Figure 3. Generated donut mode 0 in MDM-PON system.

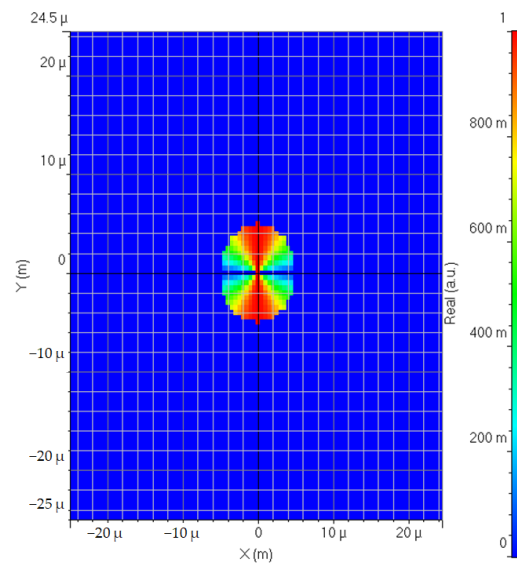


Figure 4. Generated donut mode 1 in MDM-PON system.

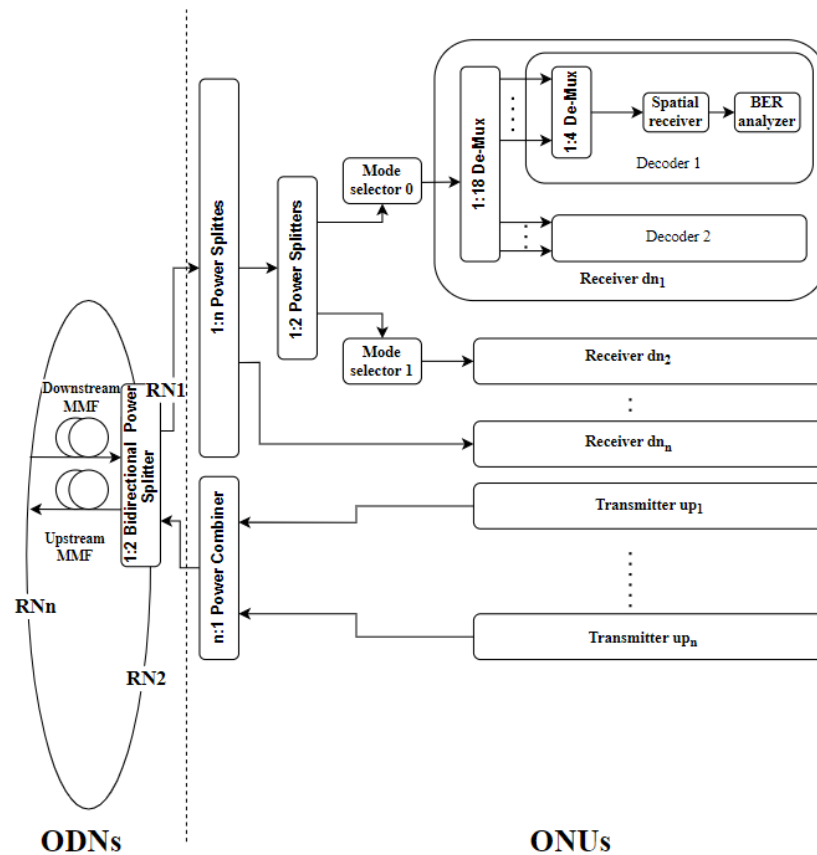


Figure 5. Proposed design of bidirectional MDM-PON system incorporating MWZCC OCDMA code of receiver section.

For data received, a 1:2 bidirectional power splitter working as RNn was utilized to split the optical data into two segments; one for the downlink receiver and another one for the uplink transmission. A 1:n power splitter was used to transmit the received traffic to separate the ‘n’ number of 1:2 power splitters. Each 1:2 splitter was utilized to split the mode signals into mode 0 and mode 1 through mode selectors 0 and 1, respectively, which select the required mode transferred at the transmitter side. Moreover, the received mode selector output is transferred to the appropriate downstream receiver section, which

includes a 1:18 de-multiplexer to de-multiplex the incoming mode signals to two decoders for decoding the output for two users. A decoder includes a 4:1 WDM MUX, which is accompanied by a spatial receiver to retrieve the basic baseband signal succeeded by the BER analyzer. For the uplink, the input signals from ‘*n*’ uplink transmitters (Tx up1 to Tx upn) are combined by an *n*:1 power combiner, which is again fed into a 1:2 bidirectional power splitter and upstream MMF. Here, for each transmitter and receiver section, eighteen upstream wavelengths of 1527–1533.8 nm with 0.4 nm channel spacing were generated at 0 dBm input power while the rest of the connections remained the same as the downlink. The system was designed and analyzed in OptiSystem 19.0 software.

Table 1 presents the MWZCC code pattern utilized in the system for two users at both donut modes 0 and 1. Moreover, Table 2 presents the assorted parameters utilized in the proposed system modeling.

Table 1. MW-ZCC code design for two users for both downlink and uplink wavelengths [37].

	λ_{dn} (nm)	1596	1596.4	1596.8	1597.2	1597.6	1598	1598.4	1598.8	1599.2	1599.6	1600	1600.4	1600.8	1601.2	1601.6	1602	1602.4	1602.8
λ_{up} (nm)	1527	1527.4	1527.8	1528.2	1528.6	1529	1529.4	1529.8	1530.2	1530.6	1531	1531.4	1531.8	1532.2	1532.6	1533	1533.4	1533.8	
U1	0	0	0	0	1	1	0	1	1	0	0	0	0	0	0	0	0	0	0
U2	0	0	0	0	0	0	0	0	0	0	0	0	0	1	1	0	1	1	1
U2	0	0	0	0	0	0	0	0	0	0	0	0	0	1	1	0	1	1	1

Table 2. Parameters used [34].

Parameters	Values
Laser input power (downlink)	10 dBm
Laser input power (uplink)	0 dBm
Wavelength (downlink)	1596–1602.8 nm
Wavelength (uplink)	1527–1533.8 nm
Data rate (downlink)	10 Gbit/s
Data rate (uplink)	2.5 Gbit/s
Reference wavelength	1550 nm
Dark current	9 nA
Measured index multimode fiber length	100–800 m
Dispersion	17 ps/nm × km
Attenuation	0.25 dB/km

3. Results and Discussion

In this segment, the results obtained from the design of the hybrid MDM-based TWDM-PON system utilizing MWZCC code are depicted and discussed for both downlink and uplink transmission considering the 10^{-3} BER threshold in OptiSystem software.

Figure 6 presents the BER performance of the 10/2.5 Gbit/s hybrid MDM-OCDMA-PON system over 1 km fiber distance for both users operating modes 0 and 1 in downstream and upstream transmission. The BER threshold of 10^{-3} by a dashed line is also displayed. It was noted that the system operating at mode 0 for User 1 in uplink transmission offers the best performance out of all modes. Furthermore, User 2 operating at mode 1 in uplink performs better than both downlink users, i.e., User 1 at mode 0 followed by User 2 at mode 1. The proposed system offers the minimum required received power of −31 and −28 dBm for User 1 and User 2, respectively, in the upstream transmission. Moreover, the minimum received power for User 1 and User 2 is −27 and −25 dBm, respectively, in the downstream direction. The measured eye patterns at −20 dBm received optical power for

both User 1 at mode 0 in both downlink and uplink directions, illustrating the successful transmission of traffic.

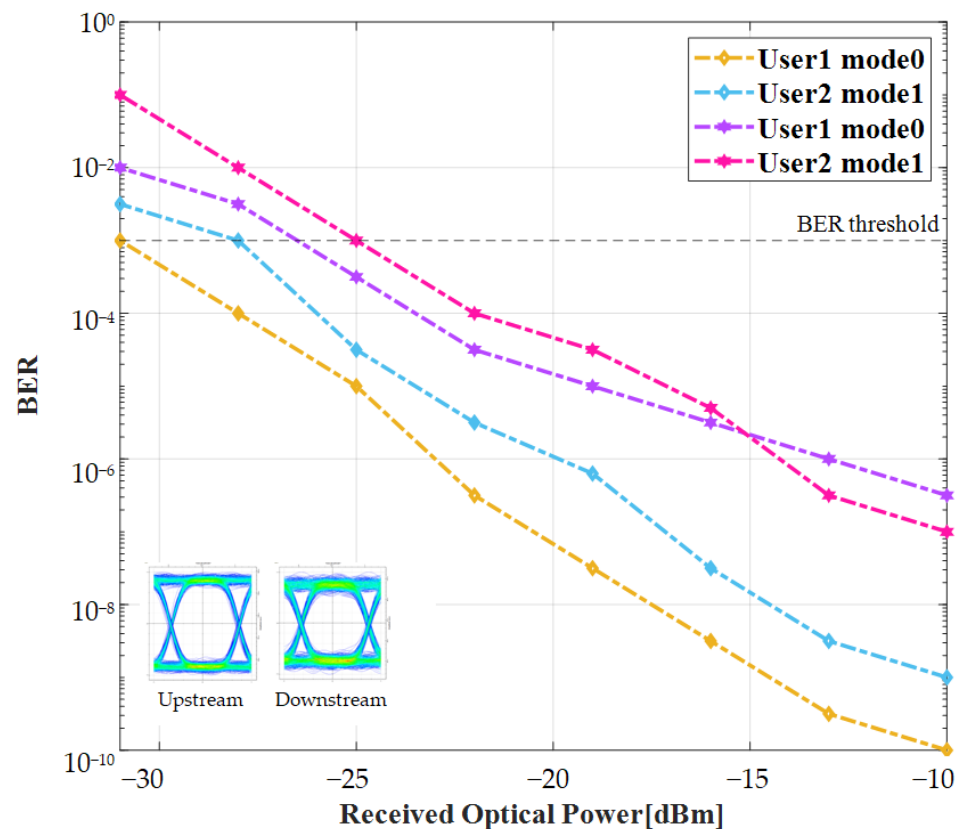


Figure 6. Measured BER vs. received optical power at 10/2.5 Gbit/s data rate over 1 km range for both User 1 and User 2 operating at modes 0 and 1 in downstream and upstream transmission. Insets: corresponding eye patterns over -20 dBm received power for User 1 operating at mode 0.

Figure 7 depicts the BER performance of the 10/2.5 Gbit/s hybrid MDM-OCDMA-PON system employing MWZCC code over 1 km fiber distance for downstream and upstream transmission, respectively, at mode 0 and mode 1 for both Users 1 and 2. It is noted that as the MMF length of fiber exceeds, the BER value increases; therefore, the system’s performance diminishes for all end users in both modes 0 and 1. Moreover, the uplink transmission performs better than the downlink as the former operates at a lesser data rate and low input power than the latter, which causes fewer impacts of fiber impairments on uplink transmission. This system performance degradation is because of the presence of non-linearities and noise in the fiber link. Moreover, User 1 operating at mode 0 performs better than User 2 operating mode 1 in both upstream and downstream transmission. It further presents that User 1 and User 2 achieve acceptable $\leq 10^{-3}$ BER at the MMF length of 1.6 and 1.3 km, respectively, in the upstream direction. Likewise, for User 1 and User 2, under the BER threshold, the obtained fiber length is 1.2 and 1 km, respectively, in the downstream direction. The computed eye patterns at the 1 km fiber range illustrate the faithful transmission of end users. MDM operates with multiple optical modes, and these modes are limited to being connected with other propagating modes because they pass through MMF. Here, mode 0 performed better than mode 1 in both downlink and uplink transmission. It is due to the reason that the traveling higher-order modes in MMF are more absorbed or scattered (due to fiber attenuation) than lower-order modes. The higher order modes (other than fundamental mode) are more susceptible to fiber bending and other variants of impact on the fiber as compared to fundamental mode (mode 0) due to the mode field cross distributions character in fiber. Additionally, the

major differential mode delay (DMD) between mode 0 and mode 1 transmission cause distributions in different operating higher-order modes. Thus, the modal dispersion caused by DMD would result in intense signal degradation at the receiver, and it restricts both the transmission distance and data rate at mode 1 than mode 0 in MMF [38,39].

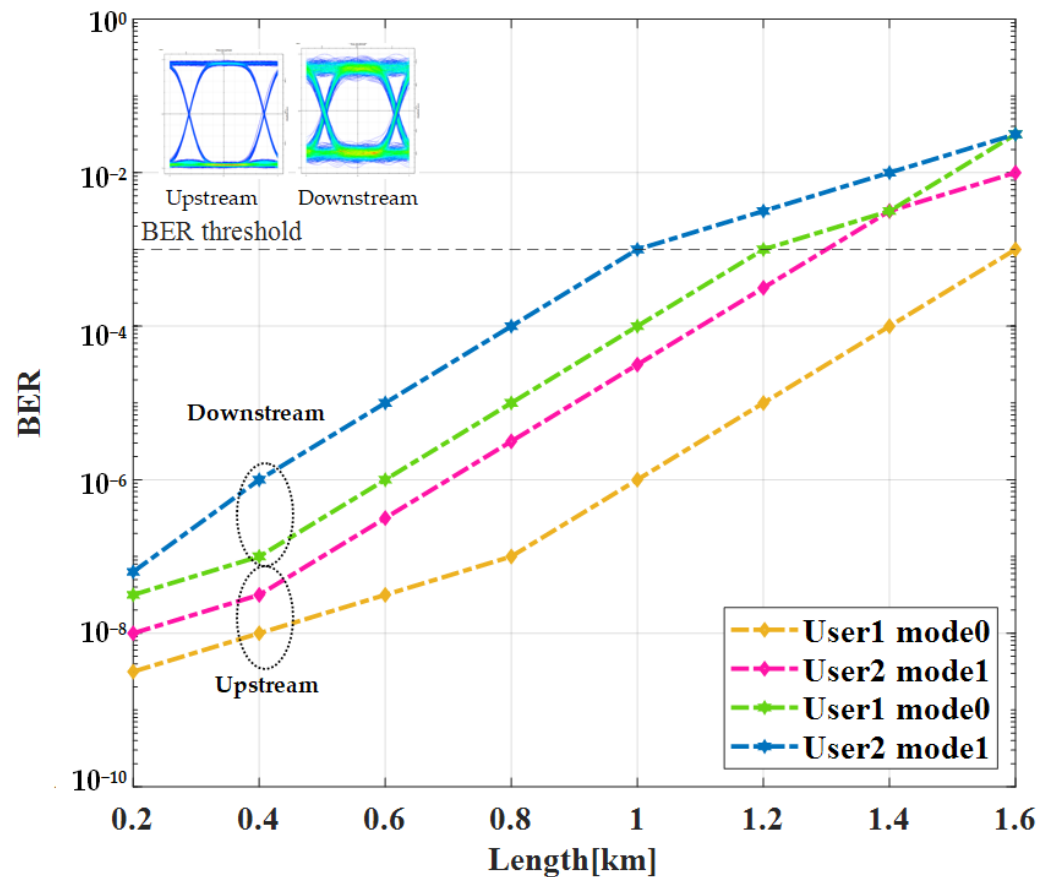


Figure 7. Measured BER vs. fiber length at 10/2.5 Gbit/s data rate for both User 1 and User 2 using modes 0 and 1 in downstream and upstream transmission. Insets: corresponding eye patterns over 1 km fiber length for User 1 mode 0.

Figure 8a,b show the measured BER performance of the 10/2.5 Gbit/s hybrid MDM-OCDMA-PON system over 1 km fiber distance for downstream and upstream transmission, respectively, at modes 0 and 1 for both users 1 and 2. It is depicted that the system operating at mode 0 offers better performance than mode 1 for both downlink and uplink transmission. For the downstream transmission operating at mode 0, it is analyzed that system using MWZCC, ZCC, RD and MD code, the minimum optical power needed to achieve the BER threshold is -30 , -28 , -22 and -20 dBm, respectively, as shown in Figure 8a. Moreover, in the downstream transmission operating at mode 1, when the MWZCC, ZCC, RD and MD codes are used in the system, the minimum received power is -20 , -14 , -13 and -8 dBm, respectively, under the BER threshold. Further, Figure 8b shows that for the upstream transmission operating at mode 0, the minimum received power for MWZCC, ZCC, RD and MD code is >-30 , -30 , -29 and -26 dBm, respectively, under the BER limit. Likewise, the power of -24 , -20 , -16 and -22 dBm was received for MWZCC, ZCC, RD and MD code, respectively, in the system for the upstream transmission operating at mode 1.

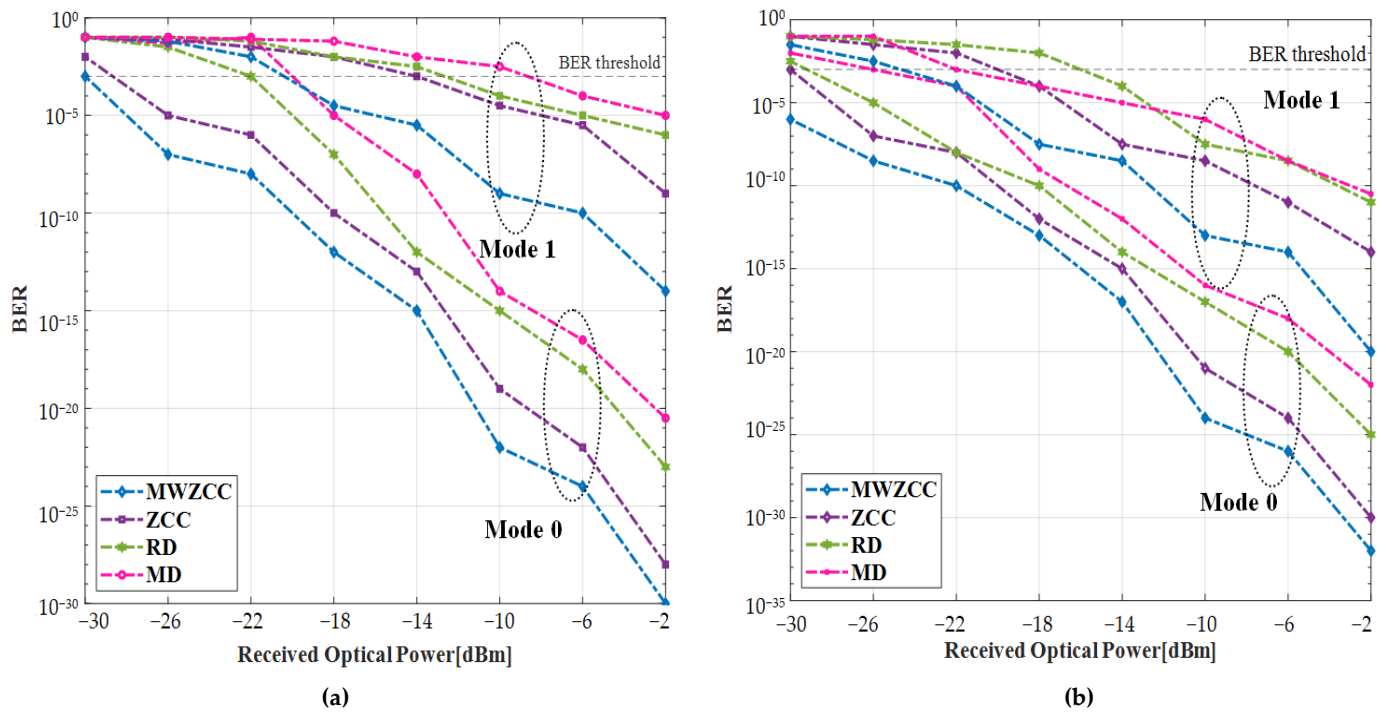


Figure 8. Measured BER vs. received optical power at 10/2.5 Gbit/s data rate over 1 km range for modes 0 and 1 for different codes in (a) downstream and (b) upstream transmission.

Figure 9a,b show the BER versus the number of active ONUs for different OCDMA codes employed in the system at 10/2.5 Gbit/s data rate over 1 km range for modes 0 and 1 for different codes in downstream and upstream transmission. It is noted that with the increasing number of ONUs, the system performance degrades along with an increase in respective BER as the received power is restricted by the power splitters for both downstream and upstream coded signals. The proposed fiber link using the MWZCC code provides superior performance with respect to the other OCDMA codes in both downlink and uplink transmission. The maximum number of ONUs obtained for mode 0 and mode 1 for MWZCC, ZCC, RD and MD code is 58, 32; 50, 24; 42, 16 and 34, 15 simultaneous ONUs, respectively, at the BER threshold in the downstream transmission as shown in Figure 9a. Additionally, Figure 9b illustrates that the maximum number of uplink ONUs handled by MWZCC, ZCC, RD and MD code is >58, 58, 50 and 44, respectively, operating at mode 0. However, in the downlink, for MWZCC, ZCC, RD and MD codes, the highest number of supported ONUs are 42, 38, 34 and 28, respectively. The performance of the proposed system for a large number of ONUs decreases because of the presence of inter-symbol interference and four-wave mixing effects, which again increases the fiber noise, non-linearities and dispersion.

3.1. Influence of FWM, Dispersion and Interference

(a) Influence of FWM: By realizing a wheel-based MDM-PON scheme utilizing MWZCC OCDMA code, the high bandwidth and secure and protected network can be obtained, but some limitations also exist in the proposed scheme. However, as the number of channels (N_c) increases in the proposed scheme, there is an increase in system capacity by N_c times, but it also causes a major non-linear effect, i.e., FWM. The FWM effect generates unwanted wavelengths because of the interference of at least three distinct wavelengths in the fiber medium. The interactions of primary wavelengths cause unwanted FWM wavelengths in the transmission link. Mathematically, the generated FWM wavelengths can be expressed as [34]:

$$\lambda_{abc} = \lambda_a \pm \lambda_b \pm \lambda_c \tag{1}$$

where λ_a, λ_b and λ_c are three primary wavelengths in the fiber link. The number of generated FWM wavelengths are expressed as [34]:

$$M = \frac{N_c^2}{2(N_c - 1)} \tag{2}$$

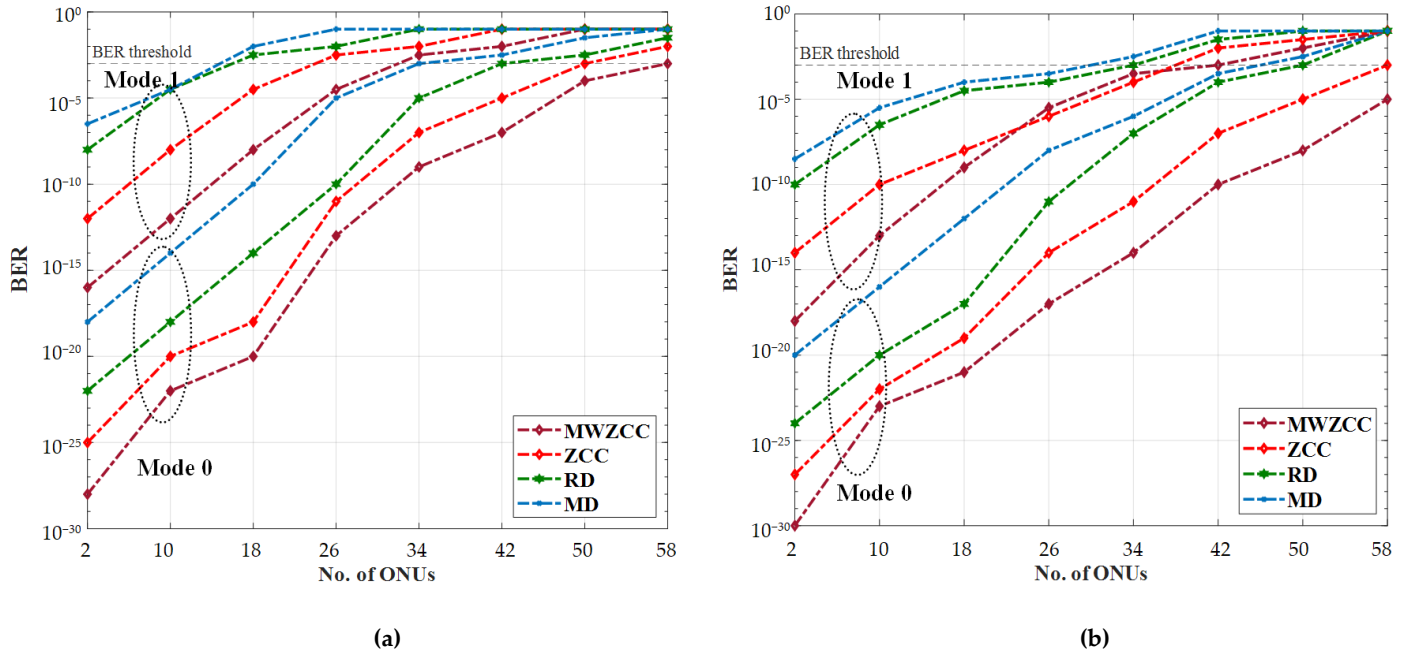


Figure 9. Measured BER vs. number of ONU's at 10/2.5 Gbit/s data rate over 1 km range for modes 0 and 1 for different codes in (a) downstream and (b) upstream transmission.

In the proposed scheme, a total of eighteen wavelengths were utilized. Thus, the total numbers of generated FWM wavelengths are 10 using Expression (2). Additionally, the decrease in channel spacing and increase in data rate in the system further increases the FWM side lobes. This impact can be minimized by using adequate channel spacing, data rate and optimum multiplexing techniques to handle multiple wavelengths. Therefore, in the proposed scheme, the MDM technique was used.

(b) Influence of Dispersion: Fiber dispersion is another parameter that decreases the system performance. However, chromatic dispersion (CD) is the main cause of restricted bandwidth in fiber. Additionally, the CD tolerance of 18,817 ps/nm and 1176 ps/nm for uplink at 2.5 Gbit/s and downlink transmission at 10 Gbit/s, respectively, is defined in [40]. Therefore, the CD present in the proposed wheel architecture, at 1550 nm reference wavelength, is calculated as [34]:

$$D_{Fiber} = L[D + S(\lambda - 1550)] \tag{3}$$

where $D_{Fiberlink}$ implies CD in fiber, L represents fiber range, λ indicates transmission wavelength, D presents dispersion coefficient and S indicates slope coefficient. Table 3 represents the calculated CD in fiber link at different transmission lengths of the proposed scheme for uplink and downlink wavelength.

The obtained results in Table 3 present that the achieved CD values are lower than the tolerance range for downlink and uplink wavelengths over 0.2~1.6 km at 10/2.5 Gbit/s data rate in the wheel-based MDM-PON with MWZCC code. However, uplink transmission shows less CD than downlink as uplink wavelength operates at a low data rate of 2.5 Gbit/s than downlink wavelength.

Table 3. Calculated CD for downlink and uplink transmission wavelengths.

Transmission	Wavelength (nm)	Length (km)	Chromatic Tolerance (ps/nm)
Downlink	1596	0.2	200
		0.6	400
		1	600
		1.2	800
		1.6	1000
Uplink	1527	0.2	150
		0.6	300
		1	450
		1.2	600
		1.6	700

(c) Influence of interference: However, for low data rate signals, the CD does not notably broaden the propagating pulses into contiguous bit periods in fiber cable. Therefore, the CD does not influence the transmission of the system at a low data rate. Furthermore, at a high data rate, the pulses are shorter and closer. It prompts pulse overlapping into neighboring bit intervals, also known as inter-symbol interference (ISI). The expression for pulse broadening in ps is given as [34]:

$$\Delta t = DL\Delta\lambda \tag{4}$$

where Δt implies pulse spread and $\Delta\lambda$ means pulse spectral linewidth, i.e., 1 nm. Additionally, the bandwidth of fiber cable is limited by dispersion and interference. Thence, the maximum supported bit rate in Gbit/s is evaluated as [34]:

$$B_r\Delta t < 1 \tag{5}$$

where B_r indicates the bit rate in the system. Table 4 indicates the measured pulse broadening and supported bit rate for distinct fiber lengths of the proposed scheme for uplink (at 2.5 Gbit/s) and downlink (at 10 Gbit/s) transmission.

Table 4. Measured pulse broadening and supportable bit rate in the proposed scheme.

Length (km)	Δt (ps)	B_r (Gbit/s) [Downlink]	B_r (Gbit/s) [Uplink]
0.2	3.4	0.03	0.008
0.6	10.2	0.10	0.2
1	17	0.17	0.4
1.2	20.4	0.20	0.5
1.6	27.2	0.27	0.6

Table 4 indicates that the supportable bit rates for both downlink and unlink transmissions are less than 1 over 0.2~1.6 km fiber length. Thus, the proposed scheme performs well under the influence of ISI.

3.2. Power Budget (PB) Analysis

PB calculates the total loss in the system due to power splitters, power combiner and mode selectors. The expression for total loss, L_T , of the system is given as [41]:

$$L_T = L_c + L_s + aL_{fiber} + L_{MS} \tag{6}$$

where L_c , L_s , a , L_{fiber} and L_{MS} represent combiner loss, splitter loss, fiber attenuation, fiber loss and mode selector loss, respectively. In the proposed system, mode selector loss is considered zero as its basic function is to draw a single mode from the multimode signal in MMF. Table 5 presents detailed loss calculations of the proposed scheme at an input power of 10 dBm and 0.2 dB/km attenuation.

Table 5. Analysis of loss budget in the proposed scheme.

Length (km)	Fiber Loss αL_{fiber} (dB)	2:1 Power Combiner (dB)	1:2 Power Splitter (dB)	Total Loss (dB)
0.2	3.4	0.3	3.6	7.3
0.6	10.2	0.3	3.6	14.1
1	17	0.3	3.6	20.9
1.2	20.4	0.3	3.6	24.3
1.6	27.2	0.3	3.6	31.1

Table 5 illustrates that the maximum engagement to the total loss in the proposed scheme is fiber loss, followed by splitter loss and connector loss. Table 6 presents the comparison of the proposed scheme with previously reported schemes.

Table 6. Comparisons of proposed scheme with other reported schemes.

Scheme	Maximum Transmission Distance (km)	Highest Data Rate (Gbit/s)	No. of ONUs	Code Used	Design Features
Hybrid tree-ring topology-based radio over fiber system [42]	26	1.25	4	Not used	Complex and costly
Ring-based WDM system [43]	60	2.5	10	Not used	Not scalable, losses and not secure
Ring-based WDM system [44]	15	10	6	Not used	Not scalable, losses and not secure
WDM Ring network [45]	10	2.5	4	Not used	Not scalable, losses and not secure
Ring-based hybrid PON-FSO [34]	10 (fiber) and 40 (FSO)	1000	50	Single weight ZCC	Not scalable, costly and more losses
Proposed scheme	1.6	10/2.5	58	MNZCC	Scalable and fewer losses

Table 6 presents that the proposed scheme based on wheel topology offers the highest number of connected ONUs (=58) with high security by employing MNZCC code with high scalability and fewer losses at a high data rate (=58 × 10/2.5 Gbit/s) than other existing schemes. Except for reference [34], no other scheme uses code for enhancing the system security at high data. Although the transmission distance of the proposed scheme is less than other schemes, other ring/tree-based schemes include losses and lack in scalability as well as security of the system. Furthermore, to improve the transmission distance and data rate in the proposed schemes, amplifiers can be employed successfully.

4. Conclusions

In this work, a 10/2.5 Gbit/s hybrid MDM-PON system incorporating OCDMA was designed. Donut modes 0 and 1 are utilized in the MDM scheme in both downlink and uplink transmission. The system operating at mode 0 performs better than mode 1 for MWZCC code as compared to ZCC, RD and MD code. For acceptable BER, the minimum required received power is −31 dBm in upstream and −27 dBm downstream over 1 km length at a 10/2.5 Gbit/s data rate. The faithful transmission distance of 1.6 km in uplink and 1.2 km in a downlink can be achieved at 10/2.5 Gbit/s successfully. Moreover, the MWZCC code offers minimum acceptable received power of −20 dBm in uplink and −30 dBm downlink direction for User 1 operating at mode 0. Moreover, the maximum number of ONUs handled by the system using the MWZCC code is 58 in both uplink and downlink transmission. The numerical measured influence of fiber impairments and

splitters/combiners depicts that a wheel-based scheme is a preferable approach for future networks. Moreover, it shows better outcomes than other existing schemes.

In addition, as the proposed scheme has various pros, it also poses some cons. The major benefit of the proposed wheel-based scheme is to offer reliable topology for fast access communication. It also improves the network protection from fiber break or failure and lowers the link connection failure impact from OLT to ONUs and vice-versa. Additionally, the proposed work lacks to consume surplus fiber capacity, as the channel capacity will be utilized under the link break/failure scenario. Additionally, the presence of embedded devices such as switches with OLT to control the traffic to the respective ONU is required, as in ring topology-based systems. In the future, a network resilience wheel-based OCDMA-based MDM-PON system can enhance the usage of the link under the presence of fiber break/failure, interference or dispersion.

Author Contributions: Conceptualization, M.K. and H.M.R.A.-K.; methodology, M.K., V.A. and H.M.R.A.-K.; software, M.K., V.A. and H.M.R.A.-K.; validation, M.K., V.A. and H.M.R.A.-K.; formal analysis, V.A.; investigation, V.A. and H.M.R.A.-K.; resources, M.K. and H.M.R.A.-K.; writing—original draft preparation, M.K., V.A. and H.M.R.A.-K.; writing—review and editing, M.K., V.A. and H.M.R.A.-K.; visualization, M.K., V.A. and H.M.R.A.-K.; project administration, H.M.R.A.-K. All authors have read and agreed to the published version of the manuscript.

Funding: There is no funding.

Data Availability Statement: All data are available in this paper.

Conflicts of Interest: The authors declare no conflict of interest.

References

- Zentani, A.; Zulkifli, N.; Ramli, A. Network Resiliency and Fiber Usage of Tree, Star, Ring and Wheel Based Wavelength Division Multiplexed Passive Optical Network Topologies: A Comparative Review. *Opt. Fiber Technol.* **2022**, *73*, 103038. [[CrossRef](#)]
- Róka, R.; Fajdiak, R.; Holasova, E.; Kuchar, K.; Orgon, M.; Misurec, J. Protection Schemes in HPON Networks Based on the PWFBA Algorithm. *Sensors* **2022**, *22*, 9885. [[CrossRef](#)] [[PubMed](#)]
- Bindhaiq, S.; Supa'At, A.S.M.; Zulkifli, N.; Mohammad, A.B.; Shaddad, R.Q.; Elmagzoub, M.A.; Faisal, A. Recent Development on Time and Wavelength-Division Multiplexed Passive Optical Network (TWDM-PON) for next-Generation Passive Optical Network Stage 2 (NG-PON2). *Opt. Switch. Netw.* **2015**, *15*, 53–66. [[CrossRef](#)]
- Kumari, M.; Sharma, R.; Sheetal, A. Passive Optical Network Evolution to Next Generation Passive Optical Network: A Review. In Proceedings of the 2018 6th Edition of International Conference on Wireless Networks and Embedded Systems, WECON 2018—Proceedings, Punjab, India, 16–17 November 2018; pp. 102–107.
- Gong, Y.; Gan, C.; Wu, C.; Wang, R. Novel Ring-Based WDM-PON Architecture with High-Reliable Remote Nodes. *Telecommun. Syst.* **2014**, *57*, 327–335. [[CrossRef](#)]
- Yeh, C.H.; Shih, F.-Y.; Chang, G.-K.; Chi, S. Reliable Tree-Type Passive Optical Networks with Self-Restorable Apparatus. *Opt. Express* **2008**, *16*, 4494. [[CrossRef](#)]
- Bulu, I.; Caglayan, H. Designing Materials With Desired. *Microw. Opt.* **2006**, *48*, 2611–2615. [[CrossRef](#)]
- Singh, S.; Singh, S. A Hybrid WDM Ring–Tree Topology Delivering Efficient Utilization of Bandwidth over Resilient Infrastructure. *Photonic Netw. Commun.* **2018**, *35*, 325–334. [[CrossRef](#)]
- Bala, A.; Dewra, S. Efficient Routing of Star-Ring Hybrid Topology with Optical Add and Drop Multiplexer in DWDM System. *J. Opt. Commun.* **2016**, *37*, 395–400. [[CrossRef](#)]
- Rani, A.; Dewra, S. Performance of Bus and Ring Network Topologies Based on SOA Bias Current. *J. Opt. Commun.* **2017**, *38*, 277–280. [[CrossRef](#)]
- Garg, A.K.; Janyani, V.; Batagelj, B.; Zainol Abidin, N.H.; Abu Bakar, M.H. Hybrid FSO/Fiber Optic Link Based Reliable & Energy Efficient WDM Optical Network Architecture. *Opt. Fiber Technol.* **2021**, *61*, 102422. [[CrossRef](#)]
- Kumar Garg, A.; Janyani, V.; Batagelj, B. Ring Based Latency-Aware and Energy-Efficient Hybrid WDM TDM-PON with ODN Interconnection Capability for Smart Cities. *Opt. Fiber Technol.* **2020**, *58*, 102242. [[CrossRef](#)]
- Hsu, C.-H.; Jiang, S.-Y.; Hsieh, S.-E.; Yeh, C.-H.; Lai, Y.-T.; Chen, L.-Y.; Liaw, S.-K.; Chow, C.-W. Hybrid Self-Protected Fiber-FSO WDM-PON System with Fiber Breakage Prevention. *Photonics* **2022**, *9*, 822. [[CrossRef](#)]
- Vidmar, M. Optical-Fiber Communications: Cite Components and Systems. *Inf. Midem Ljubljana* **2001**, *31*, 246–251.
- Batagelj, B.; Janyani, V.; Tomažič, S. Research Challenges in Optical Communications towards 2020 and Beyond. *Inf. MIDEM* **2014**, *44*, 177–184.
- Uzunidis, D.; Logothetis, M.; Stavdas, A.; Hillerkuss, D.; Tomkos, I. Fifty Years of Fixed Optical Networks Evolution: A Survey of Architectural and Technological Developments in a Layered Approach. *Telecom* **2022**, *3*, 619–674. [[CrossRef](#)]

17. Liu, J.; Lin, Z.; Zhu, H.; Shen, L.; Mo, S.; Li, Z.; Zhang, J.; Zhang, J.; Lan, X.; Liu, J.; et al. 1120-Channel OAM-MDM-WDM Transmission over a 100-Km Single-Span Ring-Core Fiber Using Low-Complexity 4×4 MIMO Equalization. *Opt. Express* **2022**, *30*, 18199. [[CrossRef](#)] [[PubMed](#)]
18. Sharma, A.; Kaur, S.; Nair, N.; Bhatia, K.S. Investigation of WDM-MDM PON Employing Different Modulation Formats. *Optik* **2022**, *257*, 168855. [[CrossRef](#)]
19. Chen, Y.; Li, J.; Zhu, P.; Wu, Z.; Zhou, P.; Tian, Y.; Ren, F.; Yu, J.; Ge, D.; Chen, J.; et al. Novel MDM-PON Scheme Utilizing Self-Homodyne Detection for High-Speed/Capacity Access Networks. *Opt. Express* **2015**, *23*, 32054. [[CrossRef](#)]
20. Chen, Y.; Li, J.; Zhou, P.; Zhu, P.; Tian, Y.; Wu, Z.; Zhu, J.; Liu, K.; Ge, D.; Chen, J.; et al. MDM-TDM PON Utilizing Self-Coherent Detection-Based OLT and RSOA-Based ONU for High Power Budget. *IEEE Photonics J.* **2016**, *8*, 1–7. [[CrossRef](#)]
21. Hu, T.; Li, J.; Ren, F.; Tang, R.; Yu, J.; Mo, Q.; Ke, Y.; Du, C.; Liu, Z.; He, Y.; et al. Demonstration of Bidirectional PON Based on Mode Division Multiplexing. In Proceedings of the 2016 IEEE Photonics Conference (IPC), Waikoloa, HI, USA, 2–6 October 2016; Volume 28, pp. 564–567. [[CrossRef](#)]
22. Hu, T.; Li, J.; Zhang, Y.; Li, Z.; He, Y.; Chen, Z. Wavelength-Insensitive Weakly Coupled FMFs and Components for the MDM-GPON. *IEEE Photonics Technol. Lett.* **2018**, *30*, 1277–1280. [[CrossRef](#)]
23. Ren, F.; Li, J.; Hu, T.; Tang, R.; Yu, J.; Mo, Q.; He, Y.; Chen, Z.; Li, Z. Cascaded Mode-Division-Multiplexing and Time-Division-Multiplexing Passive Optical Network Based on Low Mode-Crosstalk FMF and Mode MUX/DEMUX. *IEEE Photonics J.* **2015**, *7*. [[CrossRef](#)]
24. Wan, Y.; Liu, B.; Mao, Y.; Ren, J.; Ullah, R.; Chen, S.; Wu, X.; Bai, Y.; Song, X.; Tang, R.; et al. Chaotic Power Division Multiplexing for Secure Optical Multiple Access. *J. Light. Technol.* **2022**, *40*, 968–978. [[CrossRef](#)]
25. Chaudhary, S.; Tang, X.; Wei, X. Comparison of Laguerre-Gaussian and Donut Modes for MDM-WDM in OFDM-Ro-FSO Transmission System. *AEU Int. J. Electron. Commun.* **2018**, *93*, 208–214. [[CrossRef](#)]
26. Kumawat, S.; Kumar, M.R. A Review on Code Families for SAC—OCDMA Systems. In *Optical and Wireless Technologies*; Springer: Berlin/Heidelberg, Germany, 2020; pp. 307–315.
27. Ahmed, N.; Aljunid, S.A.; Fadil, A.; Ahmad, R.B.; Rashid, M.A. Performance Enhancement of OCDMA System Using NAND Detection with Modified Double Weight (MDW) Code for Optical Access Network. *Opt. Int. J. Light Electron Opt.* **2013**, *124*, 1402–1407. [[CrossRef](#)]
28. Ortiz-Ubarri, J. New Asymptotically Optimal Three-Dimensional Wave-Length/Space/Time Optical Orthogonal Codes for OCDMA Systems. *Cryptogr. Commun.* **2020**, *12*, 785–794. [[CrossRef](#)]
29. Sarangal, H.; Singh, A.; Malhotra, J.; Chaudhary, S. A Cost Effective 100 Gbps Hybrid MDM—OCDMA—FSO Transmission System under Atmospheric Turbulences. *Opt. Quantum Electron.* **2017**, *49*, 184. [[CrossRef](#)]
30. Jellali, N.; Najjar, M.; Ferchichi, M.; Rezig, H. Three-Dimensional Multi-Diagonal Codes for OCDMA System. *Optik* **2017**, *145*, 428–435. [[CrossRef](#)]
31. Upadhyay, K.K.; Shukla, N.K.; Chaudhary, S. A High Speed 100 Gbps MDM-SAC-OCDMA Multimode Transmission System for Short Haul Communication. *Optik* **2020**, *202*, 163665. [[CrossRef](#)]
32. Kodama, T.; Isoda, T.; Morita, K.; Maruta, A.; Maruyama, R.; Kuwaki, N.; Matsuo, S.; Wada, N.; Cincotti, G.; Kitayama, K. Hybrid MDM/OCDM System with Mode and Code Multi-/Demultiplexers. In Proceedings of the SPIE-Next-Generation Optical Communication: Components, Sub-Systems, and Systems III, San Francisco, CA, USA, 5–7 February 2013; Volume 9009, pp. 124–130.
33. Kodama, T.; Isoda, T.; Morita, K.; Maruta, A.; Maruyama, R.; Kuwaki, N.; Matsuo, S.; Wada, N.; Cincotti, G.; Kitayama, K. Asynchronous MDM-OCDM-Based 10G-PON over 40 km-SMF and 2 km-TMF Using Mode MUX/DeMUX at Remote Node and OLT. In Proceedings of the Optical Fiber Communication Conference, OFC 2014, San Francisco, CA USA, 9–13 March 2014; p. W2A-9.
34. Kumari, M.; Arya, V. Design of Ring—Based 1 Tbps Hybrid PON—FSO Fault Protection System Using Add/Drop Multiplexer. *Opt. Quantum Electron.* **2023**, *55*, 124. [[CrossRef](#)]
35. Kumari, M.; Sheetal, A.; Sharma, R. Performance Analysis of Symmetrical and Bidirectional 40 Gbps TWDM-PON Employing m-QAM-OFDM Modulation with Multi-Color LDs Based VLC System. *Opt. Quantum Electron.* **2021**, *53*, 1–29. [[CrossRef](#)]
36. Dutt, S.; Arya, V. The presence of compassion satisfaction, compassion fatigue, and burn—Out among the general population. *Inf. Sci.* **2022**, *4930*, 111–122.
37. Seyedzadeh, S.; Agapiou, A.; Moghaddasi, M.; Dado, M.; Glesk, I. Won-Ocdma System Based on Mw-Zcc Codes for Applications in Optical Wireless Sensor Networks. *Sensors* **2021**, *21*, 539. [[CrossRef](#)]
38. Wu, Z.; Li, J.; Tian, Y.; Ge, D.; Zhu, J.; Ren, F.; Mo, Q.; Yu, J.; Li, Z.; Chen, Z.; et al. Fundamental-Mode MMF Transmission Enabled by Mode Conversion. *Opt. Commun.* **2018**, *410*, 112–116. [[CrossRef](#)]
39. Svistunov, D.V. Selective Mode Excitation: A Technique for Advanced Fiber Systems. In *Optical Fiber and Wireless Communications*; InTechOpen: London, UK, 2017; pp. 105–122.
40. Collings, B.; Heismann, F.; Lietaert, G. Reference Guide to Fiber Optic Testing. *Jdsu* **2007**, *1*, 139.
41. Kachhatiya, V.; Prince, S. Downstream Performance Analysis and Optimization of the next Generation Passive Optical Network Stage 2 (NG-PON2). *Opt. Laser Technol.* **2018**, *104*, 90–102. [[CrossRef](#)]
42. Li, C.Y.; Chang, C.H.; Lin, Z.G. Hybrid Ring-and Tree-Topology Rof Transmission System with Disconnection Protection. *Photonics* **2021**, *8*, 515. [[CrossRef](#)]

43. Pires, J.J.O. Constraints on the Design of 2-Fiber Bi-Directional WDM Rings with Optical Multiplexer Section Protection. In Proceedings of the 2001 Digest of LEOS Summer Topical Meetings: Advanced Semiconductor Lasers and Applications/Ultraviolet and Blue Lasers and Their Applications/Ultralong Haul DWDM Transmission and Networking/WDM Compo, Copper Mountain, CO, USA, 30 July–1 August 2001; pp. 13–14.
44. Park, S.B.; Lee, C.H.; Kang, S.G.; Lee, S.B. Bidirectional WDM Self-Healing Ring Network for Hub/Remote Nodes. *IEEE Photonics Technol. Lett.* **2003**, *15*, 1657–1659. [[CrossRef](#)]
45. Sun, X.; Chan, C.K.; Wang, Z.; Lin, C.; Chen, L.K. A Single-Fiber Bi-Directional WDM Self-Healing Ring Network with Bi-Directional OADM for Metro-Access Applications. *IEEE J. Sel. Areas Commun.* **2007**, *25*, 18–24. [[CrossRef](#)]

Disclaimer/Publisher’s Note: The statements, opinions and data contained in all publications are solely those of the individual author(s) and contributor(s) and not of MDPI and/or the editor(s). MDPI and/or the editor(s) disclaim responsibility for any injury to people or property resulting from any ideas, methods, instructions or products referred to in the content.